Proc. Natl. Acad. Sci. USA
Vol. 92, pp. 5406–5410, June 1995
Biophysics

Complex flexibility of the transforming growth factor β superfamily

(conformational analysis/protomer assembly)

GANESH VENKATARAMAN*, V. SASISEKHARAN†, CHARLES L. COONEY†, ROBERT LANGER*†, AND RAM SASISEKHARAN*‡

*Harvard-Massachusetts Institute of Technology Division of Health Sciences and Technology and †Department of Chemical Engineering, Massachusetts Institute of Technology, Cambridge, MA 02139

Contributed by Robert Langer, December 30, 1994

ABSTRACT **The transforming growth factors β (TGF-βs) are important modulators of growth and differentiation. They are intermolecular disulfide-bonded homodimeric molecules. The monomer fold has a conserved cystine knot and lacks a hydrophobic core. The biological specificity of a given member of the family is believed to be determined by the conformational flexibility of the variable loop regions of the monomer. The monomer subunit assembly in the dimer is stabilized mainly by hydrophobic contacts and a few hydrogen bonds. Since these interactions are nondirectional, we examined subunit assemblies of TGF-β by using conformational analysis. The different subunit assemblies in TGF-β2 dimer were characterized in terms of the intersubunit disulfide torsion. Our analyses show that the subunit assemblies fall into two states: the crystallographically observed *gauche* + conformation and the previously not reported *gauche* − conformation, both having almost identical interaction energies. Furthermore, there is significant flexibility in the subunit assembly within the *gauche* + and the *gauche* − states of the disulfide bond. The monomer subunit assembly is independent of the variations about the loop regions. The variations in the loop regions, coupled with flexibility in the monomer assembly, lead to a complex flexibility in the dimer of the TGF-β superfamily. For the TGF-β superfamily, the cystine knot acts as a scaffold and complex flexibility provides for biological selectivity. Complex flexibility might provide an explanation for the diverse range of biological activities that these important molecules display.**

The transforming growth factors β (TGF-βs) and related polypeptides are among the most versatile signaling molecules, regulating cell growth, differentiation, migration, and death, and expression of extracellular matrix (1–4). The extended family participates in early embryogenesis in mammals in modulating growth and development (2). Some molecules in the family play a critical role in the formation of cartilage and bone, while others facilitate wound repair by regulating the expression of the extracellular matrix components (3). The range of biological activities of this growth factor family has created interest in potential therapeutic applications for TGF-β-like molecules in the treatment of a variety of conditions including scarring, retinal tears, macular holes, myocardial infarction, and bone fractures (2).

Progress has recently been made in the identification, isolation, and characterization of TGF-β-like factors and their receptors and in the characterization of their mechanism of signal transduction (4). More than two dozen TGF-β-like factors have been identified in the extended family, and five different isoforms of TGF-β itself have been described and characterized with different and overlapping biological activities (2). The biologically active forms of the TGF-β family are disulfide-linked dimers, containing subunits of 110–140 amino acids (1). All family members show sequence similarity to the prototype TGF-β1, with a unique feature of seven highly conserved cysteine residues (5). The crystal structure of TGF-β2 reveals that six of the cysteines form a defined subunit structure known as the cystine knot (6–10). Four β-strands extend from the knot, with an overall shape of fingers of a left hand, with an α-helix extended opposite to the fingers like the heel of the palm (6-9) (Fig. 1). The seventh cysteine forms an intermolecular disulfide bond with the corresponding cysteine of the second monomer subunit. The extended conformation of the monomer subunit is unique in that there is no hydrophobic core that is characteristic of globular proteins, suggesting that the only stable form of the molecule in solution is a dimer (7–9). The crystal structure indicates that the dimer is stabilized by extensive noncovalent interactions (6, 9). The subunits are related by two-fold symmetry about the intermolecular disulfide linkage at Cys-77 (6–9). Solvent molecules in the hydrophilic pocket around the disulfide linkage provide additional stabilization energy by forming hydrogen bonds bridging the monomers. Although the dimer associations are not explicitly characterized in the NMR study of TGF-β1, the unusual fold of the monomer as well as the dimer interface appear to be conserved (11). In fact, the structure of the monomer of TGF-β2 determined by x-ray crystallography and the NMR structure of TGF-β1 are almost identical (11). Sequence-variations in the loop regions and the side-chain conformations about this overall monomer fold are thought to account for the differences in the biological activity between TGF-β1 and TGF-β2 (1, 11). It is generally accepted that monomer structure is well conserved in the superfamily (9, 10). Further, on the basis of the conserved intrachain disulfide and the high three-dimensional–one dimensional profile scores of these molecules, it was predicted that the mode of dimerization

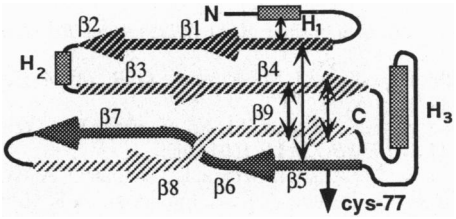

FIG. 1. Schematic representation of the primary and secondary structure of TGF-β2 monomer. Double-headed arrows denote intramolecular disulfide linkages constituting the cystine knot motif. The regions that form the exposed hydrophobic surfaces in the monomer are labeled as β-sheets 1–8 and the α-helix H_3. H_1 and H_2 are the other α-helices, and N and C correspond to the N- and C-terminal regions.

The publication costs of this article were defrayed in part by page charge payment. This article must therefore be hereby marked "*advertisement*" in accordance with 18 U.S.C. §1734 solely to indicate this fact.

Abbreviation: TGF-β, transforming growth factor β.

‡To whom reprint requests should be addressed at: E17-424, Massachusetts Institute of Technology, Cambridge, MA 02139.

in the superfamily is most likely to be head-to-tail (antiparallel) like that observed in TGF-β2 (9).

The subunit assembly in the dimer of TGF-β2 is stabilized by noncovalent interactions such as hydrophobic contacts and a few hydrogen bonds (6, 8–10). Since these interactions are nondirectional, conformational modeling studies to examine the existence of equi-energetic subunit assemblies, other than the crystallographically observed one, become important. In the TGF-β family, different subunit assemblies can be brought about by changes in the conformation of the intermolecular disulfide bond. The interaction energies in these alternate subunit assemblies were compared to the crystallographically observed assembly for TGF-β2. The effect of varying the nonconserved side chains of the monomers was also investigated to extend this analysis to other members of the superfamily.

METHODS

Molecular modeling was performed on a Silicon Graphics Iris Indigo workstation with INSIGHT II (Biosym Technologies, San Diego). Energy calculations were performed by using DISCOVER force field in vacuum (dielectric of 1.0).

A cystine molecule was built by using the biopolymer module of INSIGHT II. The torsion about the S—S bond was varied in steps of 10° from 0° to 350° and the van der Waals and electrostatic energies were calculated at each step. The energies were normalized with the number of residues and plotted on an arbitrary scale as a function of the S—S torsion. A range of allowed conformations was obtained by using a cutoff value of 2–3 kcal (1 kcal = 4.18 kJ)/mol per residue above the minimum energy (12). Additional residues were added to the C and the N termini of both the cystines and the conformational map was regenerated as described (data not shown).

The crystal coordinates of TGF-β2 were obtained from the Brookhaven Data Bank. Both the structures 1TFG.pdb (6, 7) and 2TGI.pdb (9) were used for the analysis. The two structures are not different; rms deviation of non-hydrogen atom coordinates is 0.80 Å. The dimer coordinates were generated from the monomer coordinates by applying a twofold transformation about the S—S bond. The C^{β}—S—S—C^{β} torsion was varied in discreet steps between 0° to 350° to generate the different monomer subunit assemblies. The total energy as well as the individual energy contributions were calculated at each step. The calculations were performed at shorter intervals close to minimum of the *gauche* + (*g*+) and *gauche* − (*g*−) regions of the disulfide bond. The energies were plotted as a function of the S—S torsion value. A range in the torsion values was obtained by using an arbitrary tolerance of 2–3 kcal/mol per residue above the minimum energy (12).

The main-chain and side-chain conformations of the crystallographic monomer unit (1TFG.pdb) were minimized by using 500 steps of steepest-descent algorithm followed by 500 steps of conjugate gradient. The C^{α} trace of the monomer was fixed during the minimization. This minimized monomer was almost identical to both the crystal structures (rms deviation of non-hydrogen atom coordinates between minimized monomer and 1TFG.pdb is 0.184 Å, and that between the monomer and 2TGI.pdb is 0.820 Å). The possible assembly states of the TGF-β2 dimer obtained by using crystallographic monomer coordinates or the minimized monomer coordinates were found to be identical. Any variations in the conformation of the loop regions did not affect the possible assembly states.

Another set of calculations, where the side chains of the dimer molecules are minimized at each step of S—S torsion, were performed. At each of the assembly states, the side chains of both the subunits were allowed to vary, keeping the C^{α} trace of the subunits fixed. At each step, the minimized dimer coordinates and those obtained by using a twofold symmetry about the S—S bond were almost identical (rms deviation of non-hydrogen atom coordinates is less than 0.2 Å). The total energy was plotted as a function of the disulfide torsion. A range in torsion values was obtained, using an arbitrary cutoff of 2–3 kcal/mol per residue from the minimum energy. The minimized dimer structure corresponding to the S—S torsion of 80° is almost identical to the crystallographic dimer structure (1TFG.pdb). The other crystal structure (2TGI.pdb) is almost identical to the minimized dimer structure corresponding to the S—S torsion of 88°.

Solvent-accessible surface area was calculated by using the solvation module in INSIGHT II with a probe radius of 1.4 Å (13, 14). The interfacial contact area of residues in the dimer was calculated as the difference between the solvent-accessible area of a residue in a monomer and in the dimer. The stabilization energy was determined by using a conversion of about 20 cal/mol·$Å^2$ of interfacial contact (15–17). Hydrogen bonding interactions were determined by using the algorithm in INSIGHT II.

Mutations of the amino acid sequences were performed by using the biopolymer module in INSIGHT II. The sequence of TGF-β1 was used in the TGF-β2 structure. Keeping the C^{α} trace fixed, the main chain and the side chain conformations were minimized. The subunit assemblies for the TGF-β1 molecule were determined as described earlier.

RESULTS

The conformation about a disulfide linkage in general has been known to be restricted to *trans*, *g*+, or *g*− states (18). However, when cystines are flanked on the N and the C termini by any other amino acid, our calculations show that the disulfide bond conformation is restricted to *g*+ or *g*− states. The *trans* conformation is eliminated because of steric hindrance of the flanking peptides. This conformational preference is conserved when the amino acid chains are extended in the N or C terminus and folded, although the exact locations and the flexibility within the *g*+ or the *g*− state depend on the overall protein folding as well as the side-chain interactions.

Consistent with the above analysis, our conformational energy calculations show that the intermolecular disulfide bond in TGF-β2 can also adopt the *g*+ and *g*− conformations. When the crystallographic coordinates (nonminimized) were used, the range of the *g*+ region was found to be limited to 10°, centered at 79° for 1TFG.pdb and at 88° for 1TGI.pdb. The range in the *g*− region is restricted to 30° and is independent of the crystal structure coordinate set used in the analysis. Also, the above ranges are identical, if the minimized monomer subunit coordinate set is used. The restricted nature of these ranges arises due to steric contact at the interface of the subunits. However, minimizations of the dimer (as described in *Methods*) significantly increases the range of the *g*+ region to 60° and *g*− region to 40° (see Fig. 2). The ranges of allowed conformations (shown in Fig. 2) seem to be controlled entirely by the van der Waals repulsive forces arising from steric contact between the backbones of the two monomer subunits. The electrostatic contribution does not change in these ranges (Fig. 2).

The minimized monomer subunit conformer and the two crystallographic conformations of the monomer (6, 9) are nearly identical except for differences in the loop regions. The network of disulfide bridges that is characteristic of this family preserves the monomer scaffold (9, 10). The crystallographically observed dimer of TGF-β2 corresponds to the *g*+ state of the disulfide linkage, with the intermolecular disulfide torsion at either 79° (1TFG.pdb) or 88° (2TGI.pdb). The difference in the disulfide torsion values of the two crystal structures could arise from the difference in the resolution of the x-ray data. Interestingly, the calculated minimum energy assembly in the *g*+ state is around 80° (Fig. 2). The monomer subunits are oriented in an antiparallel fashion (head to tail) in this state and the dimer interface is stabilized by hydropho-

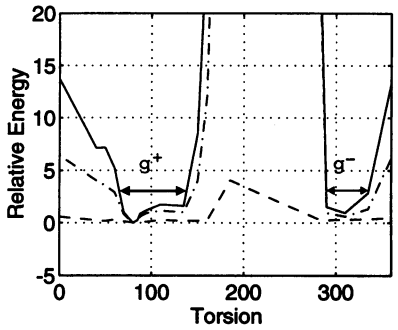

FIG. 2. Conformational energy diagram for the different assembly states of TGF-β2. The minimized monomer coordinates were used. The monomer subunit assemblies are represented by the intermolecular disulfide torsion angle (°) and the conformational energy is normalized with the number of residues (kcal/mol per residue) and is plotted relative to the minimum energy. The total energy (—) shows two distinct minima corresponding to the $g+$ and $g-$ conformations. The flexibility within each conformational state was determined by using a tolerance of 3.0 kcal above the minimum energy and is represented by (⟷). The range in the $g+$ region is from 70° to 130° and in the $g-$ region is from 290° to 330°. The global minimum energy assembly (occurring at S—S torsion angle of 80°) is similar to the crystallographically observed assemblies for TGF-β2. The electrostatic component (– – –) of the energy does not vary for the different assembly states. The van der Waals component (– · –) controls the total energy. Mutations in the sequence of amino acids do not affect the overall features of this energy profile.

bic contact between the helix H_3 and β-sheets β2–β3, β6–β7, and a few hydrogen bonds.

Subunit Assembly at $g+$ Region. As shown in Fig. 2, the monomer subunit assembly has a flexibility of 60° about the S—S bridge. In this region, the total hydrophobic contact area does not change significantly, although the actual residues that participate depend on the precise orientation of the subunits. For instance, in the crystallographic dimer, the C terminus of the helix H_3 is exposed, while the middle and the N-terminal region of this helix is in interfacial contact with the β-sheets of the other subunit (Fig. 3). Helix H_3 moves parallel to the plane of the β-sheets when the conformation of the S—S bond is varied. At assemblies corresponding to lower torsion values (70° to 80°), the C-terminal region of the helix is brought into the dimer interface, making contact with β2 and β3. The N-terminal region of the helix moves closer to β6–β7 and the end residues are pushed out of the interface into the solvent. Hence there is a small increase in the overall hydrophobic contact area. However, steric hindrance between the β6–β7 and the N-terminal region of the helix H_3 restricts further rotation in this direction. There is no steric hindrance to rotation in the opposite direction, wherein the helix H_3 moves out of the interface. In this situation, the N-terminal region of the helix H_3 moves toward β2–β3 while β-sheets β6–β7 are left exposed to solvent (Fig. 3 *Lower*).

The change in the overall solvent-accessible area in the $g+$ assemblies is less than 10%. Specifically, at the disulfide torsion value of about 70°, the subunit assembly is such that Tyr-65, Ile-68, Asn-69, Ala-72, and Ser-73 of helix H_3 are in contact with the Asp-27, Leu-28, and Trp-30 of β3. In addition, residue Ser-102 (in β7) is also brought into interfacial contact, while residues Thr-56 and Gln-57 are pushed out of the interface and exposed to solvent (Fig. 4). On the other hand, at higher S—S torsion values (80° to 130°), the residues at the end of the helix H_3 (Ile-68 and Ala-74) become fully accessible to solvent. Moreover, the residues in the middle of the helix are also more exposed (Fig. 3), as a result of the sliding of the helix outside the interface. The trend in the change of solvent accessibility at higher torsions is similar to that observed in the crystal structure of 1TGI.pdb. Residues in the loop connecting β2 and β3 (residues Ile-22 and Leu-28) as well as some residues in the

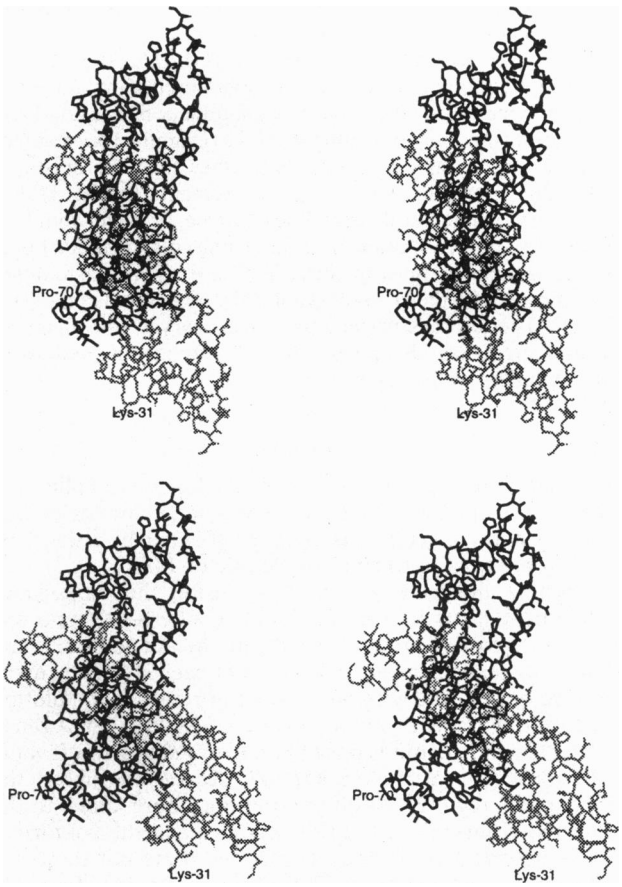

FIG. 3. Stereo diagram comparing x-ray crystal assembly of TGF-β2 (*Upper*) and the monomer subunit assembly corresponding to disulfide torsion of 110° (*Lower*). Note the change in the relative orientation of the subunits. The residues at the interface for the crystallographic dimer are as follows: Leu-20, Ile-22, Asp-27, Leu-28, Trp-30, Phe-43, Thr-56, Gln-57, His-58, Val-61, Leu-62, Leu-64, Tyr-65, Ile-68, Ala-74, Cys-77, Val-79, Leu-83, Leu-101, and Asn-104. In *Lower*, of the residues mentioned for *Upper*, residues Asp-27, Trp-30, His-58, Val-61, Tyr-65, Ile-68, Ala-74, and Asn-104 become more exposed to solvent. In addition, residues Asp-55, Lys-60, Gln-81, Asp-82, Asn-103, and Lys-110 are more buried at the interface. Hydrogen bonds between the subunits in *Upper* are as follows: His-58 $H^{\varepsilon 2}$ to Asn-42B O; His-58 HN to Asn-103B O; His-58B $H^{\varepsilon 2}$ to Asn-42 O; and His-58B HN to Asn-103 O. In *Lower* they are Gln-57B HN to Tyr-39 O (side chain); Gln-57 HN to Tyr-39B O; Ser-80 H^{γ} to Ser-112B O^{γ}; and Ser-80B H^{γ} to Ser-112 O^{γ}.

β-sheet β6 (residues Cys-77, Cys-78, and Leu-83) are buried in the interface for this entire $g+$ assembly state. Note that these residues are highly conserved in the TGF-β family (7).

In addition to the hydrophobic contacts between the subunits, the crystal structure is stabilized by hydrogen bonds, both directly between the subunits and also bridged through intervening solvent molecules (see legend to Fig. 3 and ref. 9). There are four direct hydrogen bonds between the two subunits in 1TFG.pdb. The main-chain N of His-58 is hydrogen bonded to the main-chain O of Asn-103 of the symmetrical subunit; the side-chain $N^{\varepsilon 1}$ of His-58 is hydrogen bonded to the main-chain O of Asn-42. These hydrogen bonds are not broken for a 4° rotation about the S—S bridge on either side of the crystallographic value. At torsion values higher than 83°, these hydrogen bonds are broken but alternate hydrogen bonds are formed (see legend to Fig. 3). At lower values of the torsion (close to 70°), there are no direct hydrogen bonds between the subunits. The hydrogen bonds bridged through water were not included in these calculations. The number of solvent molecules at the interface, as determined by the solvent-accessible area, does not change for these assemblies.

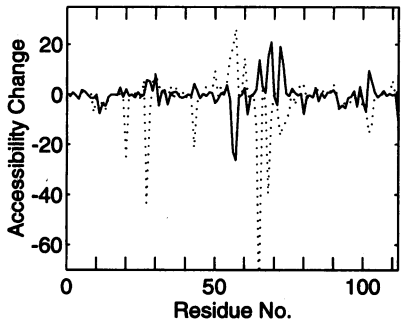

FIG. 4. Change in solvent accessibility of TGF-β2 residues at different assembly states. The difference between the solvent accessibility of a particular residue in the TGF-β2 crystal dimer and that in a different assembly state is plotted as a function of the residue number. Two different assemblies are shown: (*i*) S—S torsion of 70° (—) and (*ii*) S—S torsion of 110° (···). A positive ordinate value indicates that the residue is more accessible to solvent in the crystallographic dimer than in the altered association state. The residue is more exposed in the new assembly if the ordinate is negative. The solvent-accessible area for the monomer unit is 7166 Å^2. The solvent-accessible area for the crystallographic subunit assembly is 11,840 Å^2, while the accessible areas (in Å^2) at the different torsions are as follows: 70°, 11,744; 80°, 11,823; 95°, 12,236; 110°, 12,463; and 135°, 12,353. The accessible area change is less than 10% for this entire range.

Subunit Assembly at *g*− Region. The present conformational energy calculation predicts that the *g*− state, which to our knowledge has not been reported earlier, is energetically equally plausible. In the *g*− state, the molecules adopt a parallel orientation with the α-helices H_3 of the two subunits interacting with each other (Fig. 5). The β-sheets of the two subunits appear V-shaped and more solvent accessible than in the *g*+ region. In this orientation, the interfacial contact between the subunits is predominantly between the side chains along one face of the helix H_3 with a similar face of this helix on the other subunit. There is a flexibility of about 40° in the S—S bond for the association of the monomers in the *g*− state, wherein the helices H_3 of the two subunits slide past one another. Different residues along the helical face are brought into contact as a result of these different associations. The contact area for the *g*− assembly state is significantly less than that of the *g*+ assembly state. Typically, the contact areas are about 600 Å^2 per monomer, representing a 50% decrease in the overall contact between the subunits. Hydrogen bonding between the residues in the N-terminal loop (residues 10 and 11) with the loop connecting β2 and β3 is also observed in this state.

Nonconserved Sequence Effects on Monomer Assembly. There is about 70% sequence identity between TGF-β1 and TGF-β2. To investigate the significance of nonconserved amino acid side chains on the flexibility of the subunit assembly in the dimer, we substituted the sequence of TGF-β1 in the structure of TGF-β2. Different subunit associations in the TGF-β1 dimer were then generated as described earlier. The range of subunit assemblies for TGF-β1 is found to be the same as that of TGF-β2. The lowest-energy assembly occurs in the *g*+ state and corresponds to the minimum energy assembly of TGF-β2. The structural variations in the loop regions did not alter the range of flexibility of the subunit assembly. Proline substitutions in the main chain were individually checked for the allowed φ–ψ torsions in the backbone. The amino acids at the proline mutation sites have φ–ψ torsions that are allowed for prolines—hence proline mutations were possible without any undue strain on the protein backbone. The lack of any side-chain contribution to the energy profile was confirmed by using Ala at the mutation sites. This Ala mutant also had a conformational map almost identical to that of TGF-β2.

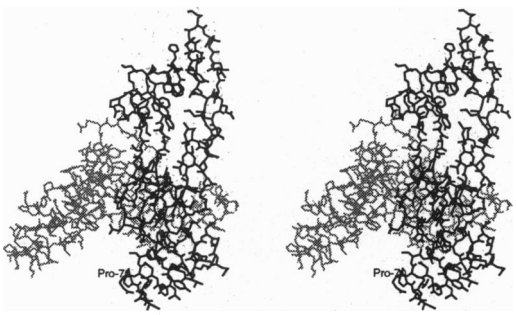

FIG. 5. Stereo diagram of the monomer assembly of TGF-β2 in *g*− conformation. Residues Asn-10, Val-11, Leu-20, Leu-28, Phe-43, Ala-45, Leu-62, Ser-63, and Thr-67 are at the interface of the two monomer units. Hydrogen bonding between the N-terminal loop with the loop connecting β2 and β3 also stabilizes this assembly.

DISCUSSION

We have shown that, over a range of 60° in the *g*+ state of the intersubunit disulfide torsion in TGF-β, the subunit associations in the dimer have similar interaction energies, hydrophobic contacts, and hydrogen bonding. This gives rise to a significant flexibility in the subunit assembly within the *g*+ state, where the x-ray crystal structure of TGF-β2 is also observed. Furthermore, our analysis suggests yet another subunit assembly corresponding to the *g*− state, with conformational energy equivalent to that of the *g*+ state. The high solvent accessibility and the easily reducible nature of the Cys-77 disulfide might establish an equilibrium between these two subunit assembly states (8). The range of flexibility for the subunit assembly as well as the minimum-energy assembly state is independent of the amino acid side-chain conformations as well as the primary sequence and depends only on the overall main-chain fold of the subunit. In spite of low sequence similarity in the superfamily (≈30% identity), the conserved cystine knot motif acts as a scaffold to preserve the main-chain fold for the superfamily (7, 9–11). Our conformational analysis, when extended, indicates that the range of flexibility for the subunit assembly as well as the minimum-energy assembly state would be the same for all the members of the TGF-β superfamily. The flexibility in the monomer assemblies for all the members of the TGF-β superfamily changes significantly the relative position and orientation between the putative receptor-binding domains, resulting in a spectrum of unique dimer surfaces.

The conformational variations of the nonconserved loop regions in the subunits are believed to provide the biological specificity for the members of the superfamily (11, 19, 20). The conformations as well as the characteristic surface properties in the loop regions of the subunits are determined by the primary sequence (11). The variations in the loop regions, coupled with the flexibility in the subunit assembly, lead to a complex flexibility in the dimer of the TGF-β superfamily. This complex flexibility in TGF-β provides for a range of structurally related proteins with unique properties. The dimer surface in these structurally related proteins is determined by both the amino acid sequence at the loops and the subunit assembly state. As a consequence, for the superfamily, the complex flexibility would confer unique binding properties and biological specificity to the dimer surface. While the disulfide bond provides additional stability to the subunit assembly for some members of the superfamily, the complex flexibility for other members that lack the intermolecular disulfide is brought about by variations in the monomer assembly in the dimer.

Although the minimum-energy assembly for TGF-β2 obtained from our calculations coincides with the crystal mono-

mer subunit assembly, in light of TGF-β's complex flexibility, it is unclear if this assembly is the only biologically significant conformer. Note that the TGF-β family is encoded as a larger precursor that remains biologically inactive until processed and activated (5). As the precursors in the TGF-β family share little homology, it remains to be seen if processing of latent TGF-βs is a possible assembling strategy (due to complex flexibility), which takes place before the formation of the disulfide bond linking the two subunits into a discrete dimer configuration. TGF-βs are known to interact with three receptors (I, II, and III) and several other extracellular matrix molecules (1). It has been proposed that TGF-β binds directly to receptor II, and this complex recruits receptor I, leading to the formation of a ternary association between TGF-β and receptors II and I, resulting in signal transduction (4). TGF-β is able to bind or recruit receptor I only upon binding to receptor II. However, it is unknown whether receptor I binds a receptor II-induced conformationally modified TGF-β or a TGF-β/receptor II complex (4). The complex flexibility in TGF-β thus raises the possibility that a particular assembly state is driven, stabilized, or modulated by its interaction with other molecules in a given environment, such as its binding to a matrix molecule. This is also consistent with the fact that TGF-β's biological activity is dependent on the cellular environment (5). The model of complex flexibility of the TGF-β superfamily described here provides a means not only for a given member of the superfamily to achieve a wide range of biological properties but also for the ability of isoforms within a family to have overlapping activities.

Starting with the crystal structure of TGF-β2, mutant TGF-β molecules have been designed with unique biological activities (19–21). Site-directed mutations or deletions of the residues in the loop regions of TGF-β1 confer altered biological activities to these mutants (19). Chimeric molecules also have been designed by swapping domains between TGF-β2 and TGF-β1 (20, 21). Understanding the complex flexibility of these proteins might enable one to rationally design mutants.

We thank Drs. M. Nugent and G. Waksman for their suggestions and critical comments. This work was supported by funds from National Institutes of Health (GM 26698) and from National Science Foundation through the Biotechnology Process Engineering Center, Massachusetts Institute of Technology.

1. Border, W. A. & Noble, N. A. (1995) *Sci. Am. Sci. Med.* **2** (1), 68-77.
2. Roberts, A. B. & Sporn, M. B. (1993) *Growth Factors* **8,** 1-9.
3. Kingsley, D. M. (1994) *Genes Dev.* **8,** 133-146.
4. Wrana, J. L., Attisano, L., Wieser, R., Ventura, F. & Massague, J. (1994) *Nature (London)* **370,** 341-347.
5. Roberts, A. B. & Sporn, M. B. (1991) in *Peptide Growth Factors and Their Receptors,* eds. Roberts, A. B. & Sporn, M. B. (Springer, Berlin), pp. 419-472.
6. Schlunegger, M. P. & Grutter, M. G. (1993) *J. Mol. Biol.* **231,** 445-458.
7. Schlunegger, M. P. & Grutter, M. G. (1992) *Nature (London)* **358,** 430-434.
8. Daopin, S., Piez, K. A., Ogawa, Y. & Davies, D. R. (1992) *Science* **257,** 369-373.
9. Daopin, S., Li, M. & Davies, D. R. (1993) *Proteins Struct. Funct. Genet.* **17,** 176-192.
10. McDonald, N. Q. & Hendrickson, W. A. (1993) *Cell* **73,** 421-424.
11. Archer, S. J., Bax, A., Roberts, A. B., Sporn, M. B., Ogawa, Y., Piez, K. A., Weatherbee, J. A., Tsang, M., Lucas, R., Zheng, B.-L., Wenker, J. & Torchia, D. A. (1993) *Biochemistry* **32,** 1164-1171.
12. Ramachandran, G. N. & Sasisekharan, V. (1968) *Adv. Protein Chem.* **23,** 283-345.
13. Lee, B. & Richards, F. M. (1988) *J. Mol. Biol.* **55,** 379-400.
14. Ooi, T., Oobatake, M., Nemethy, G. & Scheraga, H. A. (1987) *Proc. Natl. Acad. Sci. USA* **84,** 3086-3090.
15. Eriksson, A. E., Baase, W. A., Zhang, X.-J., Heinz, D. W., Blaber, M., Baldwin, E. P. & Mathews, B. W. (1992) *Science* **255,** 178-183.
16. Chothia, C. (1974) *Nature (London)* **248,** 338-339.
17. Matsumura, M., Becktel, W. J. & Mathews, B. W. (1988) *Nature (London)* **334,** 406-410.
18. Richardson, J. S. (1981) *Adv. Protein Chem.* **34,** 167-339.
19. Qian, S. W., Burmester, J. K., Sun, P. D., Huang, A., Ohlsen, D. J., Suardet, L., Flanders, K. C., Davies, D., Roberts, A. B. & Sporn, M. B. (1994) *Biochemistry* **33,** 12298-12304.
20. Qian, S. W., Burmester, J. K., Mervin, J. R., Madri, J. A., Sporn, M. B. & Roberts, A. B. (1992) *Proc. Natl. Acad. Sci. USA* **89,** 6290-6294.
21. Burmester, J. K., Qian, S. W., Roberts, A. B., Huang, A., Amatayakul-Chantler, S., Suardet, L., Odartchenko, N., Madri, J. & Sporn, M. B. (1993) *Proc. Natl. Acad. Sci. USA* **90,** 8628-8632.